The final publication is available at

https://doi.org/10.1016/j.foodcont.2020.107638

Additional Information

Non-destructive control in cheese processing: modelling of milk curdling phase kinetics by laser backscattering imaging

[1]Samuel Verdú, [2]Alberto J. Pérez, [1]José M. Barat, [1]Raúl Grau

[1]Departamento de Tecnología de Alimentos. Universidad Politècnica de València, Spain

[2]Departamento de Informática de Sistemas y Computadores, Universidad Politècnica de València, Spain

*Author for correspondence: Samuel Verdú

Address: Edificio 8E - Acceso F – Planta 0

Ciudad Politécnica de la Innovación

Universidad Politécnica de Valencia

Camino de Vera, s/n

46022 VALENCIA – SPAIN

E-mail: saveram@upvnet.upv.es

Abstract

The aim of this study was to explore the capacity of the laser backscattering imaging technique for modelling the curdling phase within cheese processing. For this purpose, three different formulas were studied modifying the solute concentration. Textural modifications of matrix during curdling were characterized by means viscosimetry and texture measurements, depending of the liquid or solid state of sample. The change of state because gelation was determined with the aim of determining the limits for the liquid and solid phases. Moreover, the process was also characterizing by imaging technique showing dependence on both, solutes concentration and enzymatic effect, into the two phases previously observed. After reducing dimensionality using multivariate statistical procedures, imaging results showed high influence of solute concentration in captured variance by imaging technique. It reduced the visibility of phase change in image parameters. Once that influence was eliminated, the evolution of matrix across liquid and solid phases could be modelled. Such data were divided by phases and used to successfully predict the status of matrix into each one using multivariate non-linear regression procedures. It was concluded that laser backscattering imaging technique presented suitable properties to be used for nondestructive continuous monitoring of curdling process within cheese making process

1. Introduction

One of the most important stages in the cheese making process is the curdling phase (Everard et al., 2007). The main objective of this phase is pass form a liquid state of milk matrix to a solid state by a progressive gelation. This can be done in two ways: either by adding enzymes (chymosin) that modify caseins structures reducing solubility, or through the reduction of pH, rising isoelectric point of proteins and then reducing the solubility. Caseins represents around 80% of protein fraction of the milk. It forms part of the milk matrix in form of dispersed clusters called micelles. These clusters are assumed as spherical structures formed by different protein subunits (α_{s1}, α_{s2}, β and κ-casein), calcium and phosphate (Harton & Shimizu, 2019). There is a heterogenic distribution of the different caseins throughout this structure. In this sense κ-casein have crucial role in the process because its hydrophilic nature. It is located principally on the surface of the micelle from where stabilizes the structures and prevents them from aggregating together (Vacca et al., 2020). Thus, the enzymatic activity during curdling phase involves modification of the hydrophilic properties of the casein micelles. Those modifications are focused on the surface via proteolysis of Phe_{105}-Met_{106} bonds of κ-casein, inducing then aggregation and a three-dimensional, space-filling gel formation. Therefore, curdling process is composed by two phases from enzymes addition: proteolysis and aggregation (Bittante et al., 2012). However, it is difficult to control the phases because aggregation overlaps the proteolysis reaction; the latter is certainly not complete before the aggregation begins. Aggregation forms bigger and bigger structures until eventually the matrix acquires the solid nature of the gel. From that moment, matrix components and enzymes retained into structural spaces reduce movement capacity but continue working to the end of gel maturation.

The kinetics of this enzymatic process involves a large number of factors that affect directly in the physicochemical properties and then quality features of the end product. Some of them are the milk origins, enzymes concentration, concentration of solutes, temperature, presence of calcium, etc (Panthi et al., 2019). The variation of these factors could affect the kinetics of the enzymes activity and then modify the optimal cutting time of the formed curd. Alterations in cutting time

could produce effects such us excessive whey loss, increases on hardness of the gel, accumulations of high amount of water, etc. Thus the knowledge of milk matrix status during curdling phase by means of control techniques is fundamental to avoid modifications in the properties of the product because variations in the cutting time.

The control and characterization of this process has been put into practice from different approaches by means in both continuous monitoring on-line and laboratory analysis applications. Most of the instrumental methods work by destructive procedures by measuring physical properties such viscosity and other textural parameters (Aldalur et al., 2019), then cause significant alterations in the milk matrix that produce difficulties in matching of measurements with the real evolution of process. In addition, these devices limit the development of other on-line applications in the cheese production chains, such us curd cutting applications (O'Callaghan et al., 2002). In this sense, several non-destructive applications have been developed for curdling process characterization, which are based in different principles such us ultrasounds (Jiménez et al., 2017), optical techniques (Arango & Castillo, 2018; Castillo et al., 2005; Mateo et al., 2010), nuclear magnetic resonance (Curti et al., 2019) and different image analysis procedures (Darnay et al., 2017). Within image analysis procedures, the laser-backscattering imaging characterizes the extinction of light transmittance across a changing magnitude measured in a given matrix. This principle has already been used to monitoring curdling process but in a classical optical turbidimetry approach (Lomholt et al., 1998) which presented limitations such as a dilute sample of milk is necessary. Laser-backscattering imaging follows that principle, but applying a more powerful light source, imaging analysis and data mining techniques for studding the diffraction patterns generated because milk matrix-light interactions. The possibilities of extracting information from continuous processes increases with these features, and then improve the knowledge of the produced phenomena. Our research group have applied this imaging technique to modelling different features in food processing and products such us predict textural properties of vegetable creams (Verdú et al., 2018), modeling the effect of fiber enrichment in properties of cookies (Verdú et al., 2019a) or characterizing antimicrobial particles with essential oils (Verdú

4

et al., 2020). Concretely, the successfully application on the non-destructive modelling of yogurt fermentation (Verdú et al., 2019b) focused our work in applying this technic for controlling other production chains within milk industry. In this sense the production of cheese has operations that have similitudes in biochemical terms and therefore presents high interest to be controlled by this technique.

Thus, the aim of this work was to study the capacity of laser backscattering imaging to continuous control and modelling of milk curdling phase kinetics in a non-destructive mode.

2. Material and methods

2.1 Sample preparation and milk curdling process

The raw materials for the curd formulas were fresh whole cow's milk (4,5% carbohydrates, 3.1% proteins and 3.5% lipids) and skimmed milk powder (54% carbohydrates, 33% proteins and 1% lipids) acquired in the local distributor. Animal rennet (chymosin 80% w/v) was acquired in Productos Nievi S.L. (Bizkaia). $CaCl_2$ was acquired from Sigma-Aldrich (Madrid-Spain). In order to obtain matrix with different properties in processing and textural terms, three different of formulations were studied. For this purpose, modifications were done in composition by modifying the amount of added skimmed milk powder. Modifications in dry matter concentration of milk produced alterations in matrix and curdling kinetics that allowed us study the capacity of the designed device to modelling the process in different conditions in composition terms. Thus three different levels of skimmed milk were added: 1%, 6% and 8% w/v (w.b). The procedure was common for all formulas and is detailed below:

1. 150 ml of fresh whole milk was heated to 40ºC with stirring

2. Addition of skimmed milk powder in the defined proportion and 0.15 g of $CaCl_2$ until complete dissolution.

3. 100mL of the mixture was divided in two cylindrical containers of thermoformed polystyrene (7cm high and 5.5cm diameter). The first container was destined to viscosity/ texture analysis, while the second one to image analysis.

4. The curdling process was started with the addition of two drops of rennet and mixing manually during 5 sec. Then samples were kept at 40ºC for 30 minutes to ensure the complete phase transition from milk to curd, following the instructions of the rennet provider. Temperature was maintained in both analysis systems by a tubular heat exchanger. Ten samples from different milk batches were prepared and analyzed for each formula.

2.2 Imaging device

To obtain continuous information from the milk curdling phase generated by the light-milk matrix interaction during the curdling process, a low-cost device consisting in a coherent light and a digital camera connected to a computer was built. Figure 1-A shows the device setup. The capture system for image analysis was a digital Logitech C920 camera with a CMOS sensor that operates at a resolution of 2304x1535. The exposure and gain settings were configured to the auto mode. The camera included an HD video working in the H.264 high quality format. Images were obtained in RPG and saved in .JPEG format with a dimension of 1980x1080. The device was placed inside a dark cabin to keep it away from light. The camera was vertically placed 15 cm over the sample surface, coupled the heat exchanger in the middle of the vision yield. The laser pointer (650 nm, 50 mW, 3 mm⌀) was perpendicularly placed 20 cm under milk container by projecting to the central zone of the bottom surface. Both the laser diode and camera were connected to a conventional computer that ran Linux. The system was controlled by a specific program that automatically triggers the camera by software to take images at a rate of 1 image/sec. for the duration of the milk curdling process (30 min). One thousand eight hundred images from each sample were obtained at the end of the curdling phase.
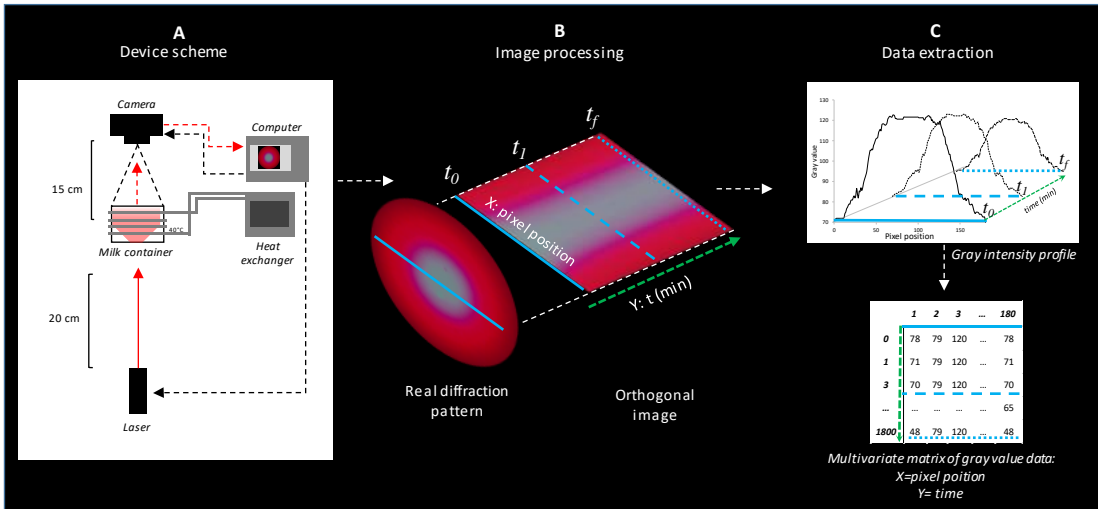
Figure 1. Scheme of device and data processing. Laser backscattering imaging device (A), image processing (B) and data extraction (C).

2.3 Image processing and data extraction

Images captured during monitoring of curdling process were the data reservoir from which to extract the information of produced changes in the milk matrix-laser interactions. The protocol for extraction of information were done by an own software. That software was based in a previous application of us, explained in Verdú et al. (2020) . It was developed in C language using the OpenCV 2.4.1 image processing libraries (Bradski, 2000) to quickly and accurately process images. It run on a computer with Linux Ubuntu 16.04 as the operating system. The protocol was run as follows:

1. Generation of an image-stack from the entire process: all images were transformed into a greyscale (8 bits) to simplify the collected information. The 1800 images captured during the curdling process were joined to an image stack, where the Y-axis represented time. The result was a three-dimensional space of pixels where the variation of diffraction patterns was collected with time (Figure 1B)

2. Orthogonal images extraction: the changes in light intensity throughout curdling process were captured in orthogonal images to simplify the monitoring process from 1800 images

to 1 image. That image was generated by slicing the stack across the time axis (Y). The size of the slice was 50 mm wide (diameter of the sample´s container), which crossed the central zone of the captured diffraction pattern (Figure 1B, continuous blue line). That wide corresponded to 180 pixels, which were assumed as single variables collecting variance of intensity by themselves. The obtained image contained the intensity profile of diffraction pattern along the X-axis at each time on the Y-axis. Thus each orthogonal image represented by itself a data matrix of changes in the intensity profiles across time.

3. Data extraction of intensity from the orthogonal images: data were extracted as gray values of each 180 variables (pixels) from the profile of diffraction pattern (X-axis) for each 1800 time captures (points of Y-axis). All extracted matrix was organized and labeled in a common data matrix with the aim of studying the evolution of each variable across time as well as the relationship with the status of the curdling process in textural terms later

2.4 Texture analysis

Measuring mechanical properties of milk during curdling process is a difficult task because the modification of matrix status in physical state terms with time. It makes difficult the use of a unique method either for fluid or solid matrix. Therefore, to interpret data obtained by imaging analysis during entire process, two methods were used to obtain data from textural status of milk matrix depending if state was either liquid or solid. During liquid phase a rotational viscosimeter was used to measure viscosity. These measurements were based on Ay & Gunasekaran (1994). Cylinder of 2cm diameter operating at 60 rpm captured shear stress in mPa.s at each second during process until arrive to phase change, indicated by a sudden increase occurred in degree of viscosity, followed by a progressive reduction. After this moment, matrix was gelated and then a TA-TX2 texture analyzer (Stable Micro Systems, Surrey, UK), equipped with a 25-kilogram load cell, was used in a no analyzed sample. A probe with a disc ($\emptyset = 35$ mm) at a constant velocity from 1 mms−1 to 50% of sample depth was used. The texture study was focused to the hardness

parameter which was represented by maximum resistance during compression, measured in g. To avoid influencing the matrix structure, samples were analyzed in the above mentioned containers at the same temperature of processing.

2.5 Statistical analysis

Physical analysis of milk matrix during processing were studied by a one-way variance study (ANOVA). In those cases in which the effect was significant (P-value < 0.05), means were compared by Fisher's least significant difference (LSD) procedure. Moreover, the data from the imaging analysis were explored after applying multivariable statistical procedures with the aim to reduce dataset dimensionality. For that purpose, the multivariate unsupervised statistical method Principal Component Analysis (PCA) was used. The objective was to simplify the analysis of variance collected by the image data matrix obtained from the continuous monitoring of curdling process. The regression studies between the curdling stage and image data was carried out by means of Support Vector Machines for regression (SVM-R). The aim of that procedure was to predict the status of milk matrix across the process from image information. SVM-R is an effective supervised learning methodology based on the statistical learning theory. This method is commonly used for multivariable data analyses (Boser et al., 1992). The used version was nu support vector regression (ν-SVM) and a polynomial function as kernel. Samples were divided by a stratified random sampling into a training batch (66% of the data) and a testing batch (33% of the data). The results were evaluated based on R^2 of prediction and error indicators: mean absolute error (MAE), mean square error (MSE) and the root mean square error (RMSE). These procedures were run with the PLS Toolbox, 6.3 (Eigenvector Research Inc., Wenatchee, Washington, USA), a toolbox extension in the Matlab 7.6 computational environment (The Mathworks, Natick, Massachusetts, USA).

5. Results and discussion

3.1 Milk curdling process

Results of texture measurements during process is showed in Figure 2. The evolution of the viscosity with time is showed in Figure 2-A, where non-differences in aggregation start times were observed but yes among the viscosity peaks of the different formulas. Viscosity started to change around 2 minutes from rennet addition. Proteolysis before that point could be active although sensitivity of device was not enough to detect it. From that time, viscosity reach with a similar slope, indicating the same velocity of gelation with independence of solute concentration. That could be done because the saturation of rennet enzymes from 1% and then generation of proteolysis without differences. Nevertheless, the max viscosity was different. The minimum one was for the 1%, while 6% and 8% had the maximum values with non-significant differences between them. From that points, viscosities were reduced systematically. In this case 8%, slower reduction was observed compared to 6%. The observed shape of viscosities evolutions was the typical response of rheological measurement of curdling process (Pazzola et al., 2018), where the end of liquid phase was marked with a peak of viscosity from which a reduction in that property was registered. That reduction is due to a leak of the liquid from gel network produced because the break of the solid structure by cylinder of viscosimeter induced share (Fernández Farrés & Norton, 2014). Thus, the viscosity registered from the peaks was due to the released of liquid phase confined into gel network, which still contain at time proteolytic activity and substrate. That could be evidenced observed the results of the texture analysis done from the observed peak viscosity. The texture of the solid gels formed from 3 minutes allowed observing the evolution of the formed network (Figure 2-B). The hardness was different at 3 min and increased to 20 min for all cases, however, in the same way of viscosity results observed previously, 6% and 8% did not presented differences. The observed increase of hardness from formed gel evidenced the overlapping of the proteolysis and aggregation phenomena (Figure 3-A), and thus the importance of the differentiation between coagulation start time and the end of curdling process.
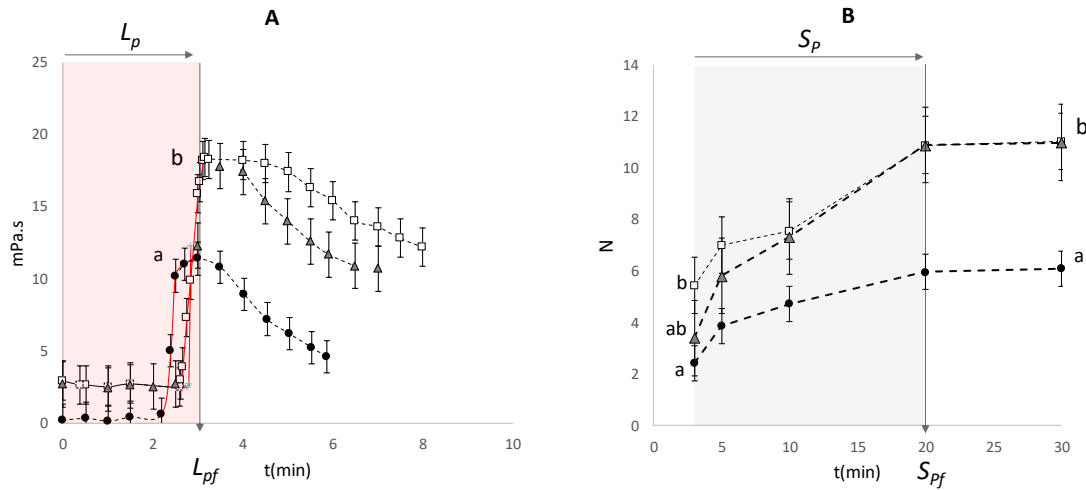
Figure 2. Viscosity and texture analysis of curdling process. A: viscosity evolution during liquid phase (L_p), B: hardness evolution during solid phase (S_p). ● 1%; ▲ 6%; □ 8%. L_{pf}: end of liquid phase; S_{pf}: end of curdling process. Watermarks indicate the observed phases for physical state of matrix. Letters marks differences at α=0.05. Bars represent standard deviation

The physical analysis of process showed then two define phases: liquid phase (L_p) where the milk matrix changed from liquid to solid state assumed until aprox. 3 minutes (L_{pf}), and solid phase (S_p) where the formed solid matrix increases the hardness because the action of enzymes in the remaining substrate from the liquid phase confined into solid network and sedimentation processes, assumed between 3-20 min (S_{pf}). From 20 min gel was assumed stable because the observed asymptotic evolution of hardness and then the end of curdling process.
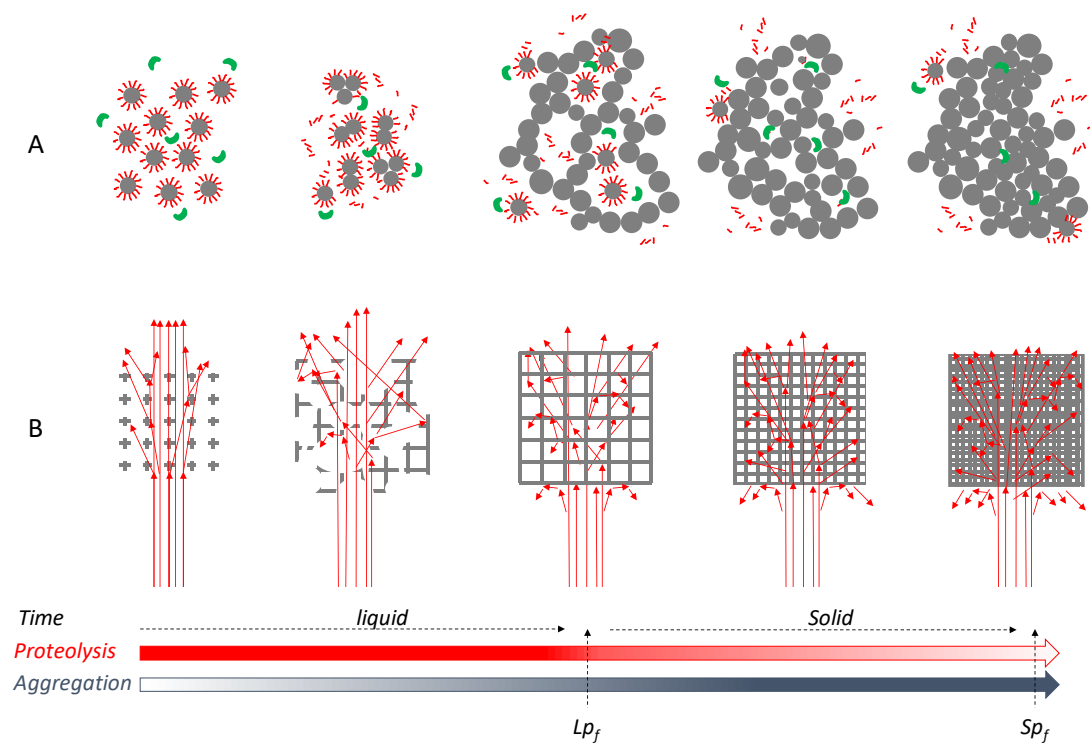
Figure 3. Proposed scheme of casein changes and laser interaction at microscopic scale across proteolysis and aggregation phenomena. A: evolution of casein micelles. B: evolution of casein network and its interaction with laser. Grey circles: casein micelles; red lines: κ-casein; green objects: enzymes; gray bars: casein network; red arrows: laser beam.

3.2 Image data exploration

In this part of the study, the image data was explored to know the influence of the two tested factors on the properties of the information collected by this technique. That information was collected from orthogonal images by each pixel in both, intensity (gray value) and coordinates terms, during entire curdling process. . Firstly, the evolution of intensity of pixels located in different positions was analyzed. Figure 4 shows the evolution of three pixels located in different zones of captured diffraction patterns. The first one was located in the middle of the saturated zone, while the other two was located at 50% and 25% of radius length respectively.

The kinetics of pixel intensities across time shows initial curve and asymptotic zone in all formulas, although differences in curve shapes were observed. It revealed how the intensity

reduced because the increasing interaction of light with casein aggregation (Figure 3-B). This phenomena match with the classical method of light backscattering to study this process in laboratory, where reduction of light transmittance was also detected in milk curdling with spectroscopic techniques (Mateo et al., 2010). However, although this fact is common for all formulas and pixels´ positions, the absolute values of intensity and their evolution were different depending of coordinates and solutes concentration. It revealed the capture of different information about process depending of the coordinates of image, which could be crucial for further studies of the process.

Thus, not only aggregation process produced reduction of intensity and modification on diffraction patterns but also the increase of solutes concentration. Increasing solutes also reduced the transmittance of laser light and then reduced the saturated zones of the captured pattern. That phenomenon produced that the properties of the image from a solid sample of 1% had higher transmitance than an image from a sample of 6% when had still liquid matrix. It was equal between 6% and 8%. That sequence can be visualized in Figure 4-A, B and C.

The observed phenomena was already observed by us when applied this imaging technique for modelling yogurt processing from different milk species (Verdú et al., 2019b). In that case, the reduction of pH by microorganisms metabolism produced the same reduction in transmittance and modifications in diffraction patterns because the precipitation of proteins. In the same way differences between milks was observed because their differences in composition in protein and lipids terms mainly. Moreover, the effect of this changes in milk matrix on other type of measurements have been also reported by Koc & Ozer (2008), who showed how casein aggregation generates a reduction on the ultrasonic attenuation coefficient of the product.
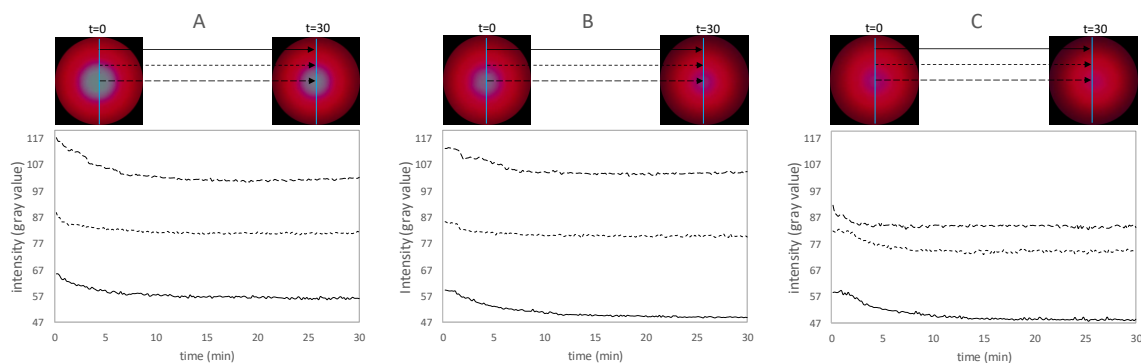
Figure 4. Evolution of different pixel locations from diffraction patterns during curdling process. A: 1%; B: 6%: C:8%. Blue line indicates the selected intensity profile.

Following the observed results about the information captured by the previous three studied pixels, the same study was done plotting all pixels the profile of diffraction pattern (Figure 5). These data were extracted from the orthogonal images (Figure 5, top right), X axis (blue) represents pixel position, Y axis represents time, and Z axis represents intensity (gray value, green dotted arrow).

The objective was to explore how the collected information from each zone of diffraction patterns evolved with different kinetics because both enzyme and composition effect, and thus to justify processing and analyzing all data from the profile of diffraction pattern. Both, time evolution of the process and solutes concentration could be differentiated visually because the differences in the evolution of each case. It revealed that the use of entire data matrix extracted from the orthogonal images captured specific variance from each formula at the same matrix modification. Therefore, orthogonal images of each sample were extracted and transformed into a multivariate data matrix with the aim of study the capability of technique for modelling the entire process.
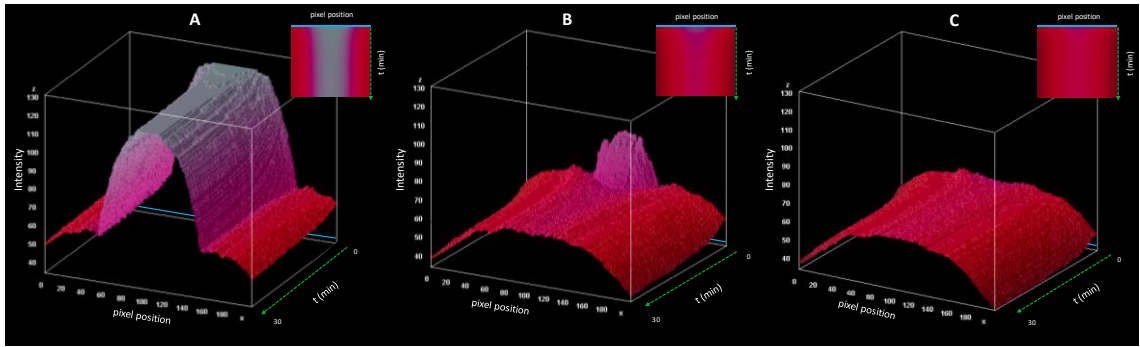
Figure 5. Evolution of the intensity profile from diffraction patterns across curdling process. A: 1%; B: 6%: C:8%. Blue line indicates the selected intensity profile. Green dotted line indicates time axis. Images in the top right zones represent the original orthogonal images.

3.3 Modelling studies

After exploring the data collected during curdling process by laser backscattering imaging, multivariate statistical procedures were applied with the aim of reduce the dimensionality of imaging datasets according to the variance captured by each pixel position across time. That reduction aimed to study the total captured variance with a reduced number of synthetic variables (PCs). Thus, a PCA was applied to the data matrix extracted from orthogonal images of all formulas. The result was a reduction from 180 variables (pixel positions of intensity profile) to one PC (PC1). This PC collected 96.1% of total variance.

Figure 6 shows the evolution of the average of scores obtained by PC1 for each formula across time. It could be observed how the variance collected by PC1 was composed by the variance produced by both, matrix evolution and solutes concentration. However, this last one had the higher variance loads as showed the differences of the scores at t=0 min. Differences in raw matter observed at t=0 followed the previous differences observed in Figure 5. The different solute concentrations generated modifications in the interaction of matrix and light which were captured in images previously to enzymatic modifications. It meant the capacity of the technique to characterizing the composition of the raw matter at the beginning of the processing. Unlike the data observed in physical analysis in Figure 2-A, the changes produced by enzymes in milk matrix

15

were detected during entire L_p, corresponding to the start of the proteolysis phenomenon. The common behavior was an increase of values from t=0 min until reaching an asymptotic progression. The main difference was observed in Lp, where an higher increase of the captured variance was observed for 6% and 8%. In Figure 6 have been marked the two observed phases in the physical analysis. L_p matched with the zone of the maximum raising for the scores, while S_p included moderated increase of scores to the asymptotic zone around t=20 min.
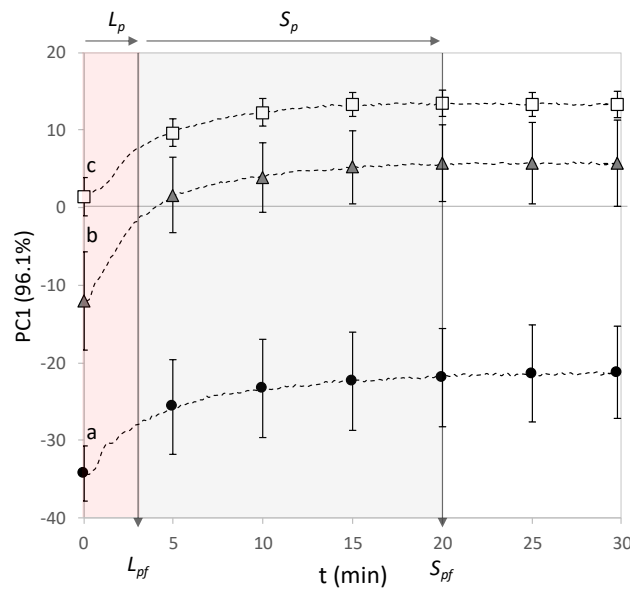

Figure 6. Kinetics of dimensionally reduced data from images collected during curdling process monitoring. ● 1%; ▲ 6%; □ 8%. L_p: liquid phase; S_p: solid phase. L_{pf}: end of liquid phase; S_{pf}: end of curdling process. Watermarks indicate the observed phases for physical state of matrix. Letters marks differences at α=0.05. Bars represent standard deviation.

Imaging data captured the variance generated into matrix during process because both proteolysis and aggregation phenomena. It meant that the differences observed in the two observed phases were collected. However, a clear change of phase was not observed within the space of variance generated by this PCA. It could occur due to the variance generated because phase change at L_{pf} point on the PC1 was diluted into the high variance load generated by the effect of solutes concentration.

For testing that hypothesis, single PCAs were done for each formula with the aim of isolating the variance contained into imaging data produced exclusively by matrix evolution across time and avoid the effect of solute concentration. The results are represented into Figure 7.
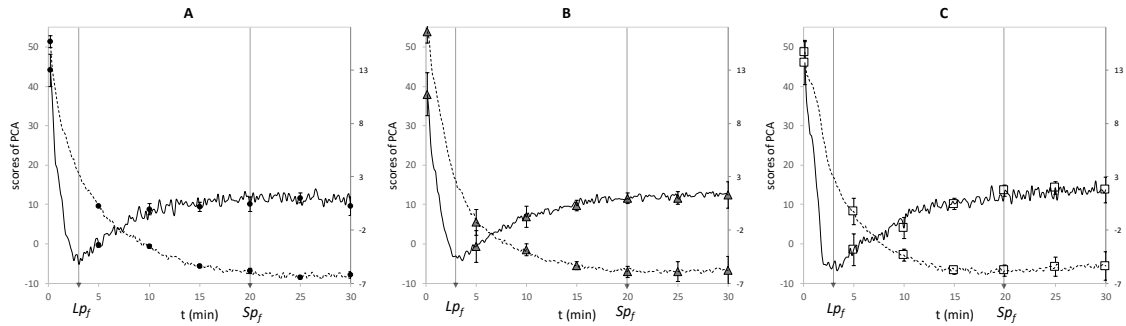

Figure 7. Kinetics of dimensionally reduced data from images collected during curdling process monitoring for single solutes concentrations. A: 1% ●; B: 6% ▲; C: 8% □. Dotted line: PC1; Black line: PC2. L_{pf}: end of liquid phase; S_{pf}: end of curdling process. Bars represent standard deviation.

The reduction of dimensionality was common for each formula, which was done in two PCs (PC1 and PC2). Those PCs cumulated more than 95% total variance in all cases. Then, in this case, total variance could be studied by two different PCs, which presented differences in their evolutions. Results showed non-differences in PCs kinetics among formulas. The plots of Figure 7 show the evolution of the average of PC1 an PC2 of each formula. The scores of PC1 (dotted lines) followed similar kinetics of the previous PCA done with all formulas simultaneously (figure 6). However, in this case both the evolution within L_p and S_p were explained into a higher scale in scores values terms. In the case of PCA of Figure 5, the evolution of L_p was explained by aprox. 10 score units while in the single PCAs (Figure 7) variance within this phase was explained by aprox. 40 score units. This fact allowed better appreciate differences between L_p and S_p, not by a marked zone but yes with a clearer slope change. Nevertheless, the evolution of PC2 showed important differences compared to PC1. In this case an important change of tendency was observed at L_{pf}, from which followed inverse evolution of PC1 until the asymptotic zone S_{pf}. The

17

differences observed in PCs in this case could be explained by the two main phenomena developed during process. Kinetics of PC1 could be better related with proteolysis activity. This phenomenon started at t=0 and evolved uninterruptedly with time until S_{pf}, following PC1 kinetics. However, the aggregation phenomenon was overlapping with proteolysis, and generated an important punctual modification when the minimum casein network for to be a solid matrix occurred. Therefore, that event could be attributed to the variance captured by PC2. The change of phase also explained the inversion of tendency for that PC.

Thus, avoiding variance produced by solutes concentration by means single PCAs, the kinetics of matrix evolution were confirmed equal for all formulas. That revealed that the times for the two previously observed phases in physical analysis were minimally altered within the used range of concentration of solutes. It was according with the explanation of the enzymes saturation, which were working at maximum velocity because an excess of substrate in all cases.

These results suggested the possibility of modelling the curdling process of studied formulas with the aim of predicting the status of each phase for each formula, or better yet, for all together. For this last case, PC1 or PC2 of each formula (Figure 7) were employed at the same time. So, models could characterize the process by means of determining L_{pf} and S_{pf} from imaging data (through PC1 or PC2 respectively). For this purpose, time was transformed to the percentage of processing (%t) to arrive at the end of each phase, it is to say L_{pf} and S_{pf}, represented 100% of L_p and S_p phases respectively. Figure 8-A shows the joined average data of scores from each formula (Figure 7) with the new units for time. It can be seen the overlapping of scores for all formulas.
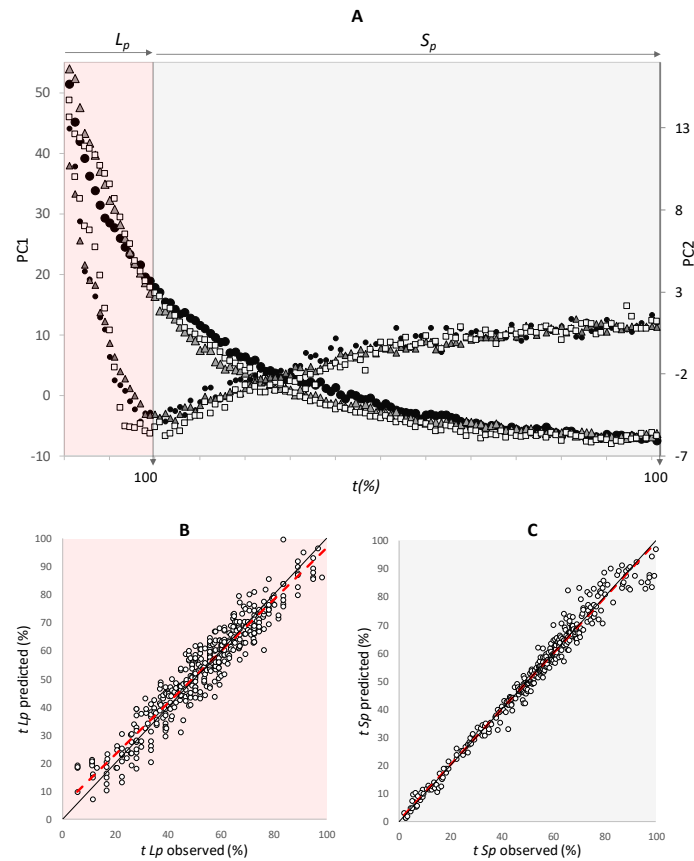
Figure 8. Regression studies. A: Overlapping of scores of PC1 and PC2 from single studies; B and C: % t observed vs. predicted from imaging data for L_p and S_p. ● 1%; ▲ 6%; □ 8%. L_p: liquid phase; S_p: solid phase.

For modelling, *SVM-R* was used due to its capacity for modelling non-linear relationships. Table 1 shows the results for prediction. The obtained R^2 were higher than 0.90 for both single and unified model and not differences in errors were observed specifically. The modelling of %t was then successfully done for both phases, although the error measurements report better results for S_p. That effect can be observed on the differences in the dispersion of the plots of measured vs. predicted data included in the Figure 8-A and 8-B. That plots correspond to the unified model. Those differences could be explained due to the properties of milk matrix during L_p. It could generate higher variability in diffraction patterns because movements of own dispersed components and formed protein flocs across the still fluidized matrix. That effect could be reduced

at L_{pf}, when matrix change to solid status and then generated more stable interactions with laser-light in despite of proteolysis and aggregation continued until S_{pf}.

Table 1. Prediction parameters for regression models between curdling status vs. imaging data.

Formula	Phase	Model parameters			
		MSE	RMSE	MAE	R^2
1%	L_p	73.54	8.114	6.046	0.931
	S_p	17.887	4.229	3.352	0.967
6%	L_p	69.146	8.315	6.615	0.933
	S_p	14.523	3.811	2.443	0.973
8%	L_p	73.012	8.545	6.598	0.927
	S_p	44.514	6.672	4.882	0.937
Unified model	L_p	68.7	8.3	6.6	0.92
	S_p	28.7	5.4	3.9	0.95

L_p: liquid phase; S_p: solid phase. R^2: Correlation coefficient observed vs. predicted; MAE: mean absolute error; MSE: mean square error: RMSE: root mean square error.

Results reported that data captured and extracted from laser backscattering imaging had high dependency of milk changes produced by both proteolysis and aggregation. It meant that and could be used to predict the status of the matrix across curdling process. That prediction could be done with independence of solute concentration within the range studied in this experiment.

6. Conclusions

The capacity of laser backscattering imaging to characterizing and modelling of milk curdling phase kinetics in a non-destructive mode was evidenced for the tested formulas in this experiment. The diffraction patterns generated because milk-matrix and laser interaction depended on both solutes concentration and curdling process status. It meant that those dependencies provided the possibility to capture variance generated by both composition features and enzyme activity. That

features allowed the continuous monitoring the changes of physical states of matrix and therefore to determine the limits of the both phases of curdling process. Transmittance was reduced with both, the increase of solute concentration and gel formation. Moreover, the kinetics of both proteolysis and aggregation phenomena were modelled when the effect of solute concentration was eliminated. The change of phase, due to the formation of the minimum gel network to be solid and its evolution, could be modelled by means of imaging data, allow us to generate accurate regression models for each phase. Those models showed accurate predictions for both single and unified approaches. Therefore, it was concluded that laser backscattering imaging technique presented suitable properties to be used as tool for nondestructive tool in the continuous monitoring of curdling process within cheese making process. New studies are being done to know the influence the factors such us of milk origins, fat fraction and different temperatures on the observed skills of technique.

7. Acknowledgment

8. Bibliography

Aldalur, A., Ong, L., Bustamante, M. Á., Gras, S. L., & Barron, L. J. R. (2019). Impact of processing conditions on microstructure, texture and chemical properties of model cheese from sheep milk. *Food and Bioproducts Processing*. https://doi.org/10.1016/j.fbp.2019.05.003

Arango, O., & Castillo, M. (2018). A method for the inline measurement of milk gel firmness using an optical sensor. *Journal of Dairy Science*. https://doi.org/10.3168/jds.2017-13595

Ay, C., & Gunasekaran, S. (1994). Ultrasonic attenuation measurements for estimating milk coagulation time. *Transactions of the American Society of Agricultural Engineers*. https://doi.org/10.13031/2013.28151

Bittante, G., Penasa, M., & Cecchinato, A. (2012). Invited review: Genetics and modeling of milk coagulation properties. *Journal of Dairy Science*, *95*(12), 6843–6870. https://doi.org/10.3168/jds.2012-5507

Boser, B. E., Guyon, I. M., & Vapnik, V. N. (1992). A Training Algorithm for Optimal Margin Classifiers. *Proceedings of the 5th Annual ACM Workshop on Computational Learning Theory*, 144–152. https://doi.org/10.1.1.21.3818

Castillo, M., González, R., Payne, F. A., Laencina, J., & López, M. B. (2005). Optical monitoring of milk coagulation and inline cutting time prediction in Murcian al Vino cheese. *Applied Engineering in Agriculture*.

Curti, E., Pardu, A., Del Vigo, S., Sanna, R., & Anedda, R. (2019). A low-field Nuclear Magnetic Resonance dataset of whole milk during coagulation and syneresis. *Data in Brief*. https://doi.org/10.1016/j.dib.2019.104520

Darnay, L., Králik, F., Oros, G., Koncz, Á., & Firtha, F. (2017). Monitoring the effect of transglutaminase in semi-hard cheese during ripening by hyperspectral imaging. *Journal of Food Engineering*. https://doi.org/10.1016/j.jfoodeng.2016.10.020

Everard, C. D., O'Callaghan, D. J., Fagan, C. C., O'Donnell, C. P., Castillo, M., & Payne, F. A. (2007). Computer vision and color measurement techniques for inline monitoring of cheese curd syneresis. *Journal of Dairy Science*. https://doi.org/10.3168/jds.2006-872

Fernández Farrés, I., & Norton, I. T. (2014). Formation kinetics and rheology of alginate fluid gels produced by in-situ calcium release. *Food Hydrocolloids*, *40*, 76–84. https://doi.org/10.1016/j.foodhyd.2014.02.005

Harton, K., & Shimizu, S. (2019). Statistical thermodynamics of casein aggregation: Effects of salts and water. *Biophysical Chemistry*, *247*(February), 34–42. https://doi.org/10.1016/j.bpc.2019.02.004

Jiménez, A., Rufo, M., Paniagua, J. M., Crespo, A. T., Guerrero, M. P., & Riballo, M. J. (2017).

Contributions to ultrasound monitoring of the process of milk curdling. *Ultrasonics*.
https://doi.org/10.1016/j.ultras.2017.01.007

Koc, A. B., & Ozer, B. (2008). Nondestructive monitoring of renetted whole milk during cheese
manufacturing. *Food Research International*, *41*(7), 745–750.
https://doi.org/10.1016/j.foodres.2008.05.008

Lomholt, S. B., Worning, P., Øgendal, L., Qvist, K. B., Hyslop, D. B., & Bauer, R. (1998).
Kinetics of the renneting reaction followed by measurement of turbidity as a function of
wavelength. *Journal of Dairy Research*. https://doi.org/10.1017/S0022029998003148

Mateo, M. J., O'Callaghan, D. J., Everard, C. D., Castillo, M., Payne, F. A., & O'Donnell, C. P.
(2010). Evaluation of on-line optical sensing techniques for monitoring curd moisture
content and solids in whey during syneresis. *Food Research International*.
https://doi.org/10.1016/j.foodres.2009.09.023

O'Callaghan, D. J., O'Donnell, C. P., & Payne, F. A. (2002). Review of systems for monitoring
curd setting during cheesemaking. In *International Journal of Dairy Technology*.
https://doi.org/10.1046/j.1471-0307.2002.00043.x

Panthi, R. R., Kelly, A. L., Sheehan, J. J., Bulbul, K., Vollmer, A. H., & McMahon, D. J.
(2019). Influence of protein concentration and coagulation temperature on rennet-induced
gelation characteristics and curd microstructure. *Journal of Dairy Science*, *102*(1), 177–
189. https://doi.org/10.3168/jds.2018-15039

Pazzola, M., Stocco, G., Paschino, P., Dettori, M. L., Cipolat-Gotet, C., Bittante, G., & Vacca,
G. M. (2018). Modeling of coagulation, curd firming, and syneresis of goat milk from 6
breeds. *Journal of Dairy Science*, *101*(8), 7027–7039. https://doi.org/10.3168/jds.2018-
14397

Vacca, G. M., Stocco, G., Dettori, M. L., Bittante, G., & Pazzola, M. (2020). Goat cheese yield
and recovery of fat, protein, and total solids in curd are affected by milk coagulation

properties. *Journal of Dairy Science*. https://doi.org/10.3168/jds.2019-16424

Verdú, S., Barat, J. M., & Grau, R. (2019a). Laser backscattering imaging as a non-destructive quality control technique for solid food matrices: Modelling the fibre enrichment effects on the physico-chemical and sensory properties of biscuits. *Food Control*. https://doi.org/10.1016/j.foodcont.2019.02.004

Verdú, S., Barat, J. M., & Grau, R. (2019b). Non destructive monitoring of the yoghurt fermentation phase by an image analysis of laser-diffraction patterns: Characterization of cow's, goat's and sheep's milk. *Food Chemistry*, *274*(July 2018), 46–54. https://doi.org/10.1016/j.foodchem.2018.08.091

Verdú, S., Pérez, A. J., Barat, J. M., & Grau, R. (2018). Laser backscattering imaging as a control technique for fluid foods: Application to vegetable-based creams processing. *Journal of Food Engineering*, *241*(May 2018), 58–66. https://doi.org/10.1016/j.jfoodeng.2018.08.003

Verdú, S., Ruiz-Rico, M., Pérez, A. J., Barat, J. M., & Grau, R. (2020). Application of laser backscattering imaging for the physico-chemical characterisation of antimicrobial silica particles functionalised with plant essential oils. *Journal of Food Engineering*. https://doi.org/10.1016/j.jfoodeng.2020.109990